A Study of the Mechanisms of Divalent Copper Binding to a Modified Cellulose Adsorbent

David William O'Connell,[1,2] Balazs Aszalos,[2] Colin Birkinshaw,[2,3] Thomas Francis O'Dwyer[1,2]

[1]*Department of Chemical and Environmental Sciences, University of Limerick, Ireland*
[2]*Materials and Surface Science Institute, University of Limerick, Ireland*
[3]*Department of Material Science and Technology, University of Limerick, Ireland*

Received 21 January 2009; accepted 23 June 2009
DOI 10.1002/app.31889
Published online 20 January 2010 in Wiley InterScience (www.interscience.wiley.com).

ABSTRACT: A modified cellulose material was prepared by grafting glycidyl methacrylate to cellulose (Cell-*g*-GMA) with subsequent functionalization with imidazole (Cell-*g*-GMA-imidazole). This latter compound was used in the adsorption of copper from aqueous solution. The mechanism of Cu(II) binding onto the cell-*g*-GMA-imidazole was investigated at the molecular level using scanning electron microscopy (SEM), Fourier transform infrared (FTIR), x-ray photoelectron spectroscopy (XPS), energy dispersive x-ray analysis (EDX) and X-ray diffraction (XRD). FTIR and Raman spectroscopy provided an insight into the extent to which perturbation of the imidazole ring occurred following adsorption of the metal while XPS spectra indicated the binding of Cu(II) ions to nitrogen atoms by the appearance of additional binding energy peaks for nitrogen on the cellulose-*g*-GMA-imidazole sample post adsorption. The EDX technique provided clear evidence of the physical presence of both the copper and sulfate on the cellulose-*g*-GMA-imidazole material post adsorption. XRD analysis further confirmed the presence of a copper species in the adsorbent material as copper sulfate hydroxide ($Cu_3(OH)_4SO_4$ - antlerite). The XRD studies further suggest that the overall extent of Cu(II) adsorption is not alone a combination of true metal chelation as suggested by FTIR, Raman and XPS, but also a function of surface precipitation of the polynuclear copper species. © 2010 Wiley Periodicals, Inc. J Appl Polym Sci 116: 2496–2503, 2010

Key words: cellulose; modification; heavy metal; adsorption; mechanism

INTRODUCTION

Unmodified cellulose has a low heavy metal adsorption capacity as well as variable physical stability. Therefore, chemical modification of cellulose can be carried out to achieve adequate structural durability and efficient adsorption capacity for heavy metal ions.[1] In particular, two main approaches have been tried in the conversion of cellulose into compounds capable of adsorbing heavy metal ions from aqueous solutions.[2] The first of these methods involves a direct modification of the cellulose backbone with the introduction of chelating or metal binding functionalities producing a range of heavy metal adsorbents.[3–6] Alternative approaches have focused on grafting of selected monomers to the cellulose backbone either directly introducing metal binding capability or with subsequent functionalization of these grafted polymer chains with known chelating moieties.[7–9]

Correspondence to: T. F. O'Dwyer (tom.odwyer@ul.ie).

Journal of Applied Polymer Science, Vol. 116, 2496–2503 (2010)

While many of the previously mentioned studies are focused primarily on quantifying the level of metal adsorbed, other research in this area has focused more specifically on elucidation of the mechanism of the metal binding process. In practice, adsorption of heavy metals is potentially a function of several mechanisms including complexation, co-ordination, chelation, ion-exchange, adsorption, physical forces, ion entrapment in the inter and intrafibrillar capillaries and spaces of the structural polysaccharide network.[10] The overall mechanistic pathway depends on the characteristics of the adsorbent, the physicochemical properties of the heavy metals and the solution interface.[11–13] A number of studies have outlined the mechanism of Cu(II) adsorption on chitosan/cellulose beads.[14,15] These authors found through the use of FTIR and XPS techniques that copper adsorption on the beads is mainly through interaction with the nitrogen atoms in chitosan to form surface complexes. Zhou et al., found that the adsorption of Pb(II) on cellulose/chitin beads could be described as complexation between Pb(II) and the nitrogen atoms in the chitin.[16] Martinez et al., studied the adsorption of both Pb(II) and Cd(II) from aqueous solutions using grape stalk.[17] Using SEM, FTIR and energy

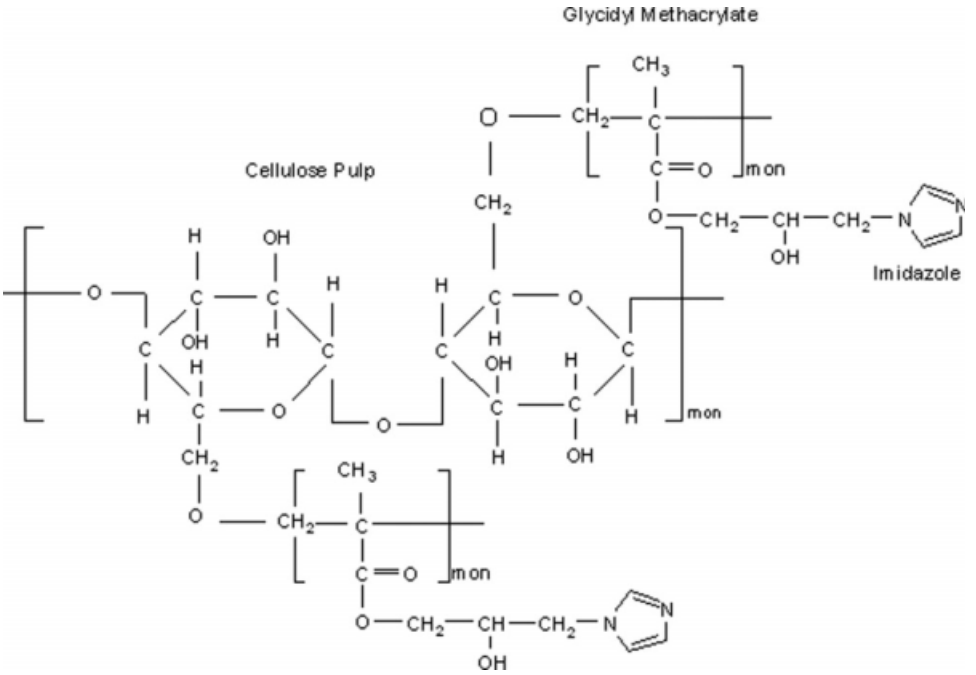

Figure 1 Structure of cellulose-*g*-GMA-Imidazole.[20]

dispersive x-ray analysis (EDX), she concluded that along with ion-exchange, other mechanisms such as surface complexation and electrostatic interaction were also involved in the metal binding mechanism. Krishnani et al., prepared a biomatrix from rice husk, a lignocellulosic waste from agro-industry, for the removal of several heavy metals as a function of pH and metal concentrations in single and mixed solutions.[18] The biomatrix was characterized using scanning electron microscopy and Fourier transform infrared spectroscopy, which indicated the presence of several functional groups for binding metal ions. Speciation of chromium, cadmium and mercury loaded on the biomatrix was determined by x-ray photoelectron spectroscopy. In similar studies, Sun et al., used the techniques of FTIR, SEM and XPS to assess the binding of several heavy metals to poly-aspartyl polymers and they found the dominant mechanism can best be described by the ion-exchange model.[19]

In our previous work we have prepared an adsorbent material by grafting the monomer glycidyl methacrylate to a cellulose backbone with subsequent functionalization of the graft with imidazole (Fig. 1). This material showed high uptake of the heavy metal Cu(II).[20] This works sets out, through the use of scanning electon microscopy (SEM), Fourier transform infrared (FTIR), X-ray diffraction (XRD) and x-ray photoelectron spectroscopy (XPS), to elucidate the mechanism of heavy metal and modified cellulose sorbent interaction at the molecular level.

METHODOLOGY

The adsorbent material, cellulose-*g*-GMA-imidazole, was prepared and characterized as outlined in our previous article.[20] Likewise, the adsorption studies for Cu(II) uptake on the prepared adsorbent was outlined in the same article. Briefly, 0.2 g of cellulose-*g*-GMA-imidazole was taken and placed in separate 25 mL plastic vials along with 25 mL of 1000 mg dm^{-3} copper(II) solutions (prepared from $CuSO_4.5H_20$ (Merck, Darmstadt, Germany). A magnetic stirrer was added to each vial with stirring for 2 h. After adsorption equilibrium, the metal loaded cellulose-*g*-GMA-imidazole was separated from the equilibrium solution by filtration and vacuum-dried at 50°C.[20] This Cu(II) loaded cellulose-*g*-GMA-imidazole sample and the unmodified original sorbent material were used in the subsequent analytical methodologies.

Scanning electron microscopy (SEM) and energy dispersive x-ray analysis (EDX)

SEM was performed using a JEOL JSM-840 electron microscope. Approximately 5–10 mg of each metal loaded cellulose-*g*-GMA-imidazole sample was scattered evenly onto the surface of an aluminium stub covered with a 12 mm diameter carbon tab. Excess solid was removed using compressed air, and the sample was sputter coated with a thin conductive film of gold before being observed and photographed.

TABLE I
Summary of Langmuir Data for Adsorption of Cu(II) on Cellulose-*g*-GMA-Imidazole[20]

Temperature (°C)	K_L ($dm^3\ g^{-1}$)	A_L ($dm^3\ mg^{-1}$)	K_L/A_L ($mg\ g^{-1}$)	R^2
7	0.5879	0.00893	65.79	0.976
23	1.5508	0.02264	68.49	0.995
40	0.4832	0.00676	71.43	0.961

EDX analysis was also performed on the JEOL JSM-840 electron microscope to analyze for the presence of copper on the cellulose-*g*-GMA-imidazole samples and also to confirm the carbon/oxygen ratios in the cellulose-*g*-GMA-imidazole material.

Fourier transform infra red spectroscopy (FTIR)

The FTIR spectra of cellulose-*g*-GMA-imidazole pre- and postmetal adsorption were recorded using a Perkin–Elmer Spectrum 2000 instrument. A 2 mg sample was mixed with 100 mg of FTIR-grade potassium bromide (KBr). The samples were scanned 30 times at 4 cm^{-1} resolution in the 4000 cm^{-1}–400 cm^{-1} range and then averaged.

X-ray photoelectron spectroscopy (XPS)

XPS analysis of cellulose-*g*-GMA-imidazole pre- and postmetal adsorption was performed using a Kratos AXIS 165 spectrometer using monochromatic Al K_α radiation ($h\nu = 1486.58$ eV) and fixed analyser pass energy of 20 eV.

X-ray diffraction (XRD)

XRD patterns of dry cellulose-*g*-GMA-imidazole samples with or without adsorbed heavy metal ions were recorded on a Philips X'pert PRO MPD instrument with nickel filtered K_α copper radiation ($\lambda =$ 1.542 Å) as the X-ray source, operated at 40 kV and a current of 35 mA between 2θ angles of 5 and 70°. Samples were ground with a mortar and pestle before analysis and pressed into a die.

RESULTS AND DISCUSSION

Cu(II) adsorption level on cellulose-*g*-GMA-imidazole

Our previous research article has outlined Cu(II) uptake levels on the cellulose-*g*-GMA-imidazole material of almost 69 mg g^{-1} at 23°C.[20] These uptake levels can be achieved in less than thirty minutes with strong Cu(II) adsorption at low equilibrium solution concentrations with an uptake plateau being reached at higher equilibrium Cu(II) concentrations. The adsorption isotherm was best described by the Langmuir model of adsorption[21] and Table I outlines the salient parameters in respect of the Cu(II) adsorption process.

Scanning electron microscopy and energy dispersive x-ray analysis

Scanning electron micrographs were used to examine and compare the surface morphology of the cellulose-*g*-GMA-imidazole and the Cu(II) loaded cellulose-*g*-GMA-imidazole samples obtained post adsorption. The SEM images are presented in Figure 2. Assessment of the SEM images reveals somewhat limited information and no clearly discernible morphological changes.

EDX analysis was then carried out on the cellulose-*g*-GMA-imidazole preadsorption and the Cu(II) loaded cellulose-*g*-GMA-imidazole samples post adsorption. The EDX spectra obtained are shown in Figure 3. These spectra indicate the presence of the adsorbed Cu(II) on the cellulose-*g*-GMA-imidazole sorbent material as evidenced by the Cu peak at 8 keV. A significant sulphur peak is also observed in

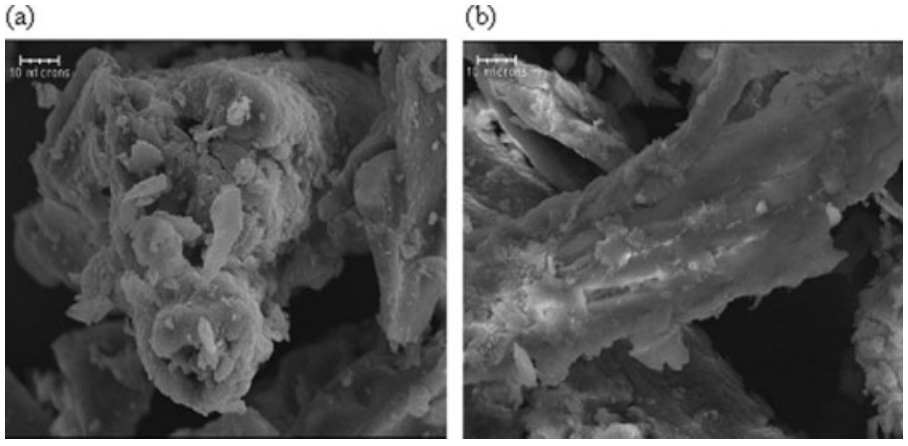

Figure 2 Comparison of the surface morphology of (a) cellulose-*g*-GMA-imidazole and (b) Cu(II) loaded cellulose-*g*-GMA-imidazole.

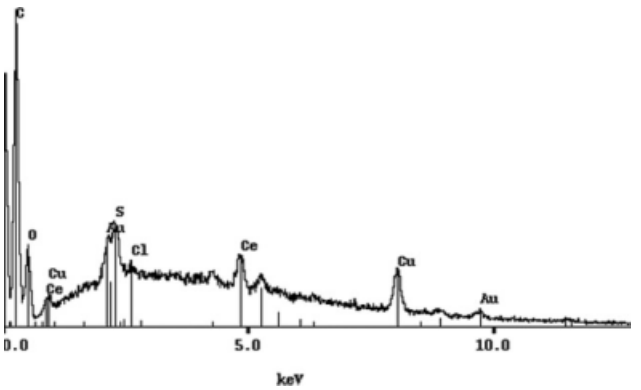

Figure 3 EDX spectra of Cu(II) loaded cellulose-*g*-GMA-imidazole.

Figure 3 and its presence may be due to sulphate anions adsorbing on the surface of the cellulose-*g*-GMA-imidazole. This is as expected since Cu(II) stock adsorbate solutions were prepared from copper(II)sulfate-5-hydrate in the first instance. Cerium is also present in EDX profile and it's presence is most likely due to residual traces of the Ce(IV) initiator used in the grafting procedure for the reaction of cellulose with glycidyl methacrylate.[20] Coupled with the results from the adsorption studies in the latter research article, the EDX plots provide clear evidence for the physical presence of the adsorbed metal on the cellulose-*g*-GMA-imidazole. The presence of sulfur in the copper plot in Figure 3 seems to suggest that along with the fundamental process of adsorption of the hexaquo cationic species, there may also exist the possibility of some level of surface precipitation of copper salts at the cellulose-*g*-GMA-imidazole/adsorbate solution interface.

FTIR analysis

To identify the possible functional groups on cellulose-*g*-GMA-imidazole involved in the binding of Cu(II), FTIR spectra were obtained before and after metal adsorption. If a ligand coordinates to a metal, the energy of the ligand material will most likely be perturbed leading ultimately to subtle shifts in the absorption peaks in the FTIR spectra. These FTIR absorption bands are usually shifted to lower or higher frequencies.[22] Figure 4 outlines the FTIR spectra of cellulose-*g*-GMA-imidazole and cellulose-*g*-GMA-imidazole-Cu(II).

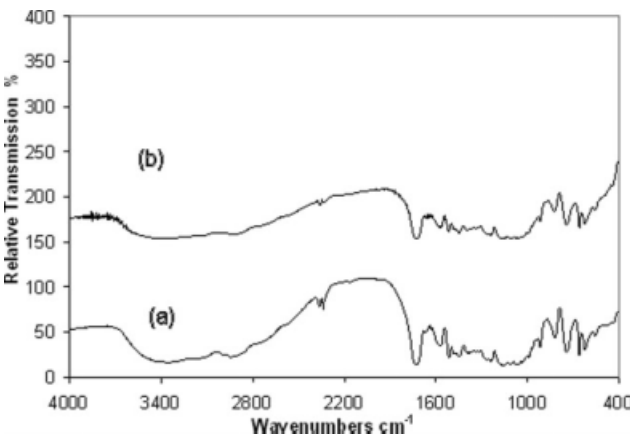

Figure 4 FTIR spectra of (a) cellulose-*g*-GMA-imidazole and (b) cellulose-*g*-GMA-imidazole-Cu(II).

TABLE II
Characteristic FTIR Peaks for Imidazole[23,24]

Functional groups	Peak wavenumber (cm^{-1})
C=C—H/N=C—H stretching	3112
Imidazole ring	1573
C—C/N—C stretching	1512
Ring vibration	1232
In plane ring C—H bending	1104

Table II summarizes the characteristic FTIR peaks normally associated with imidazole. Evidence of the presence of the imidazole ring can be seen in the FTIR spectrum of cellulose-*g*-GMA-imidazole with characteristic imidazole ring peaks occurring at 3112 cm^{-1} (C = C—H/N = C—H stretching), 1573 cm^{-1} (imidazole ring bending), 1512 cm^{-1} (C—C/*N*—C stretching), 1232 cm^{-1} (ring vibration), 1104 cm^{-1} (in-plane ring C—H bending). Peaks occurring at 1730 cm^{-1} and 1157 cm^{-1} are associated with the C—O vibration of cellulose-*g*-GMA.

A comparison of the spectra for cellulose-*g*-GMA-imidazole fibers with that of metal-loaded fibers reveals subtle changes of the major characteristic peaks for the imidazole ring. Table III summarizes the observed wavenumber shifts for the post adsorption states of the cellulose-*g*-GMA-imidazole.

There is a small shift of the ring vibration peak at 1232 cm^{-1} in cellulose-*g*-GMA-imidazole to 1235 cm^{-1} for Cu(II) loaded adsorbent. The imidazole peak at 3112 cm^{-1} due to (C = C—H/N = C—H stretching) shifts to 3104 cm^{-1} for Cu(II) loaded adsorbent. The extent of these wavenumber shifts can be taken as evidence of the interaction of the metals primarily with the imidazole ring chelation

TABLE III
A Comparison of the Wavenumber Shift for Cellulose-*g*-GMA-Imidazole with that of the Cu(II) Loaded Cellulose-*g*-GMA-Imidazole

Functional group	Adsorbent (cm^{-1})	Cu(II)-Adsorbent (cm^{-1})
(C=C—H/N=C—H stretching)	3112	3104
Imidazole ring vibration	1232	1235
Imidazole Ring (C—C/N—C)	1512	1511
Imidazole ring vibration	1573	1563

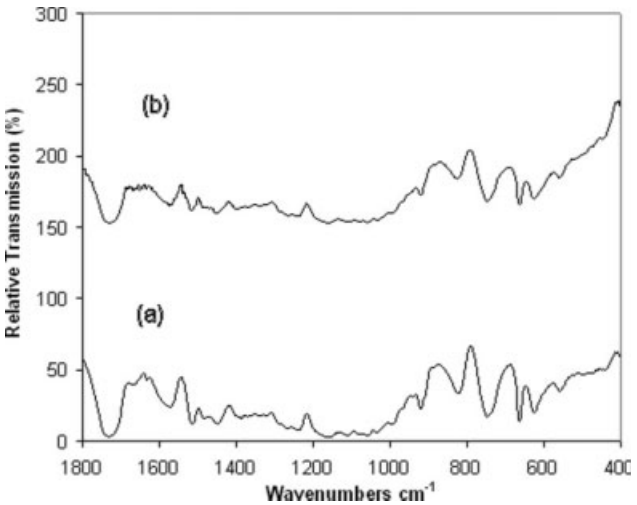

Figure 5 FTIR spectra of (a) cellulose-*g*-GMA-imidazole and (b) Cu(II) loaded cellulose-*g*-GMA-imidazole in the 1800 cm^{-1}–400 cm^{-1} region.

sites and more specifically with the nitrogens in the imidazole ring.

Figure 5 shows the FTIR spectra of cellulose-*g*-GMA-imidazole and Cu(II) loaded cellulose-*g*-GMA-imidazole in the 1800 cm^{-1}–400 cm^{-1} region. The peak for the imidazole ring at 1573 cm^{-1} shifts to 1563 cm^{-1} for Cu(II) loaded adsorbent. This band shift of the imidazole ring provides further evidence of the binding of the metal ion to the imidazole ligand in the adsorption process. It also shows the imidazole ring vibration is affected by a steric effect resulting from the incorporation of the heavy metal cation. Similar shifts have been noted in a study which focused on the interaction and mobility of Cu(II)-imidazole containing copolymer.[25] These shifts in the characteristic bands of imidazole were suggested to have occurred due to an increase in the rigidiy of the imidazole ring resulting from it's interaction with Cu(II) ions. Other research work has characterized the adsorption properties and mechanism of crosslinked carboxymethyl-chitosan resin with Zn(II) and Pb(II).[26,27] It was concluded that the carboxymethyl group, amino group, and the secondary hydroxyl group participate in the adsorption process.

Given the EDX results from Figure 3 where the presence of sulfur was established (most probably in the form of sulfate) there is a distinct possibility of metal salt surface precipitates forming on the cellulose-*g*-GMA-imidazole material. The hydrolysis of the hexaquo metal cations when at high concentrations and at increasing pH, from pH 5.5 onwards, may lead to the formation of polynuclear surface precipitates of the cation. These salts contain hydroxide species and probably sulfate anions. Evidence for the formation of these salts can be seen by the presence of hydroxide deformation modes leading to a peak at ~760 cm^{-1} in the FTIR's presented in Figures 4 and 5.

In our study, the FTIR spectra as presented offer further evidence of both energy perturbation at the imidazole ring site in the adsorbent material and the possibility of hydrolyis of the hexaquo cations leading to the possible formation of surface precipitates in addition to the normal metal chelation process.

Raman analysis

Figure 6 outlines the chemical shift in the spectra of the cellulose-*g*-GMA-imidazole and Cu(II) loaded cellulose-*g*-GMA-imidazole in the 1600–1200 cm^{-1} region. Similar to FTIR, Raman analysis was used to identify functional groups which may have been involved in the adsorption of copper. Examination of the cellulose-*g*-GMA-imidazole spectrum shows a peak at 1512 cm^{-1} which may be attributed to (C—C, C—N) in the imidazole ring.[28] This peak shifts to 1520 cm^{-1} for the Cu(II) loaded cellulose-*g*-GMA-imidazole samples. The peak at 1289 cm^{-1} which may be attributed to C—N in the imidazole ring shifts to 1283 cm^{-1} for the Cu(II) loaded cellulose-*g*-GMA-imidazole samples. These results give further supporting evidence of the nature of the binding interaction of the metal ions with the imidazole ligand during the adsorption process.

XPS analysis

XPS spectra are a useful tool in characterizing ligand effect in transition metal complexes. Electron-donating ligands will lower the binding energy (BE) of the core level electrons and electron-withdrawing ligands will raise the BE. XPS spectra are also widely used to distinguish different forms of the same

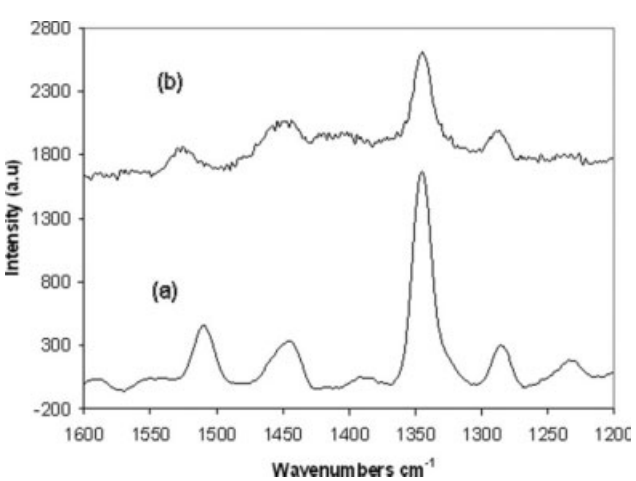

Figure 6 Raman spectra of (a) cellulose-*g*-GMA-imidazole and (b) Cu(II) loaded cellulose-*g*-GMA-imidazole in the 1600–1200 cm^{-1} region.

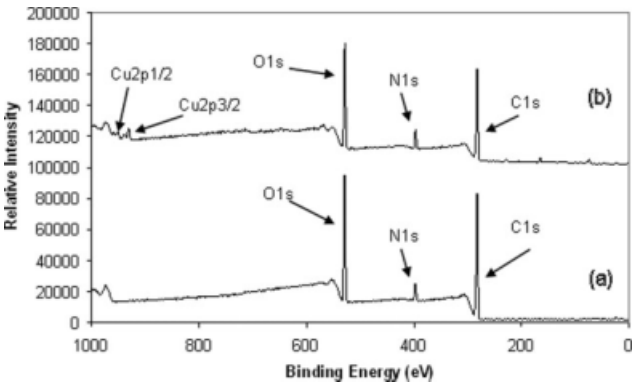

Figure 7 XPS spectra for (a) cellulose-*g*-GMA-imidazole and (b) Cu(II) loaded cellulose-*g*-GMA-imidazole.

element and to identify the existence of a particular element in a material.[29] Clear evidence for the presence of the adsorbed metal can be seen in Figure 7 which outlines the XPS spectra for the cellulose-*g*-GMA-imidazole and Cu(II) loaded cellulose-*g*-GMA-imidazole samples. In the Cu(II) loaded cellulose-*g*-GMA-imidazole samples, strong Cu 2p1/2 and Cu 2p3/2 peaks occur at 951 and 931 eV. The C1s XPS binding energy peaks for the cellulose-*g*-GMA-imidazole and the Cu(II) loaded cellulose-*g*-GMA-imidazole samples have the same carbon components indicating that the oxygen environments are similar also. It is important to note that in the O1s XPS spectra, the O1s binding energy peaks show minimal difference for cellulose-*g*-GMA-imidazole before and after metal adsorption and this indicates that oxygen atoms were most likely not intimately involved in the metal binding processes. However, as can be seen in Figure 8, there is an increase on the lower binding energy side of this range. This could be due to SO_4^{2-} sulfate anions in the case of the Cu(II) loaded adsorbent. This provides some further evidence for the probable formation of hydrolyzed

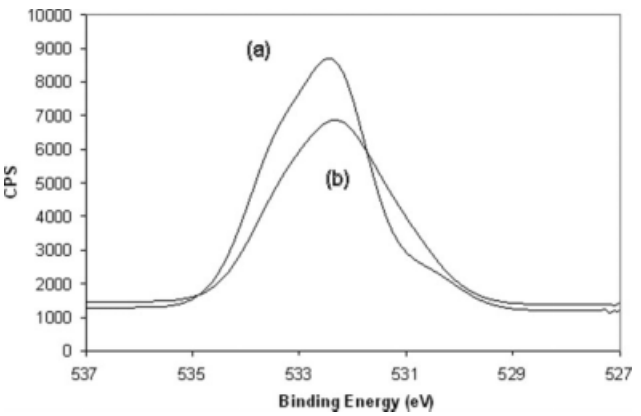

Figure 8 The O1s binding energy for (a) cellulose-*g*-GMA-imidazole and (b) Cu(II) loaded cellulose-*g*-GMA-imidazole.

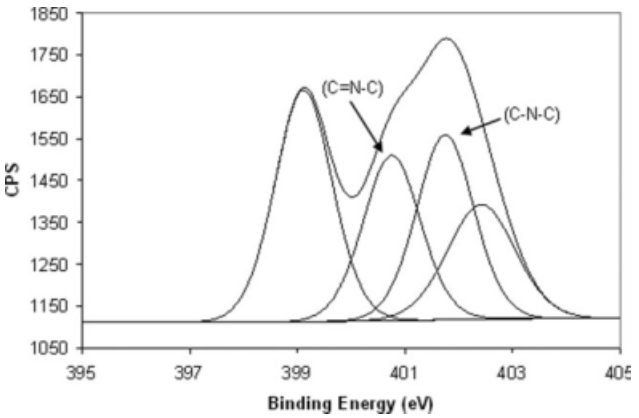

Figure 9 The N1s spectrum of cellulose-*g*-GMA-imidazole.

metal salts on the cellulose-*g*-GMA-imidazole surface.

The position of the nitrogens in the cellulose-*g*-GMA-imidazole can be observed in Figure 1. In the cellulose-*g*-GMA-imidazole XPS survey the presence of nitrogen is observed. From the N1s XPS spectra for cellulose-*g*-GMA-imidazole before metal adsorption four peaks at 399.1, 400.7, 401.7, and 402.4 eV were observed (Fig. 9). The peaks, most likely at 400.7 and 401.7 are due to imidazole.[30] In the N1s spectrum of Cu(II) loaded cellulose-*g*-GMA-imidazole these two peaks appear attributable to the imidazole component at 400.7 (C = *N*—C) and 401.7 eV (C—*N*—C) respectively. The peaks at 399.1 and 402.4 could not be identified accurately from the literature.

An additional binding energy peak appears in the N1s spectra at a different position for the Cu(II) loaded cellulose-*g*-GMA-imidazole samples. These additional peaks may be attributed to nitrogen bonding and occur at 399.51 eV for the Cu(II) sample. These different binding energy values are summarized in Table IV. Figure 10 outlines the XPS spectra of Cu(II) loaded cellulose-*g*-GMA-imidazole and specifically shows the additional binding energy peak representing the reaction of the Cu(II) ion with nitrogen in the cellulose-*g*-GMA-imidazole material.

XRD analysis

While much of the information gleaned from both the FTIR and Raman studies is concerned with the

TABLE IV
Binding Energy Values for Nitrogen Peaks in Cu(II) Loaded Cellulose-*g*-GMA-Imidazole[30]

Nitrogen peak	1	2	3
Cu(II)	401.56	400.84	399.51

perturbation of the imidazole ligand in the cellulose-*g*-GMA-imidazole adsorbent following adsorption, X-ray diffraction, alternatively, provides an opportunity to evaluate the nature of the cationic adsorbed species. The XRD patterns of cellulose-*g*-GMA-imidazole and cellulose-*g*-GMA-imidazole-Cu(II), are shown in Figure 11.

The XRD pattern of Cu-loaded cellulose-*g*-GMA-imidazole shows distinct and complex peaks at $2\theta = 13.03$, 25.92, 37.31, and 45.14°, indicating the presence of crystallized copper. This XRD profile was cross-referenced with the XRD compound library and a match was obtained corresponding to copper sulfate hydroxide or antlerite ($Cu_3(OH)_4SO_4$) which has characteristic peaks at $2\theta = 13.00$, 26.22, 37.50, and 45.25°. Antlerite is a trimeric copper species which can be formed at pH values from pH 5.5 upwards when the salt solution concentration is high.[31] The presence of this trimeric species suggests that in addition to the basic adsorption interactions, a surface precipitation mechanism also occurred in the adsorption of Cu(II) on the cellulose-*g*-GMA-imidazole.

The presence of sulfate SO_4^{2-} in the case of Cu(II) on the materials surface indicates that these anions may have a role in the cation adsorption process. Observations regarding the enhancement of metal adsorption capacity of nitrogen-type chelating adsorbents by certain anions and the deposition of these anions on the adsorbent in crystalline form has been well documented.[32] In another study, the enhancement of chitosan capacity for some transition metal ions as a result of conditioning in a sulfate-containing media before metal adsorption was investigated.[33] The improvement in metal capacity was explained as an effect of a novel crystallinity induced in the polymer in the presence of SO_4^{2-}, which allows better metal coordinating ability. Further research discussed the role of anions in suppressing high cationic charge along the chelating chain as a possible reason for the enhanced metal adsorption capacity at high anion concentrations.[34] At low pH's, it is envisaged the cellulose-*g*-GMA-imidazole will become protonated (imidazolium cation formation) reducing the affinity of the Cu(II) for binding. In the region from pH 2.0 to 4.0, competition for adsorption on the cellulose-*g*-GMA-imidazole between protons (H^+) and the Cu(II) ions exists. Uptake of the Cu(II) ions is ~50–60% of the expected maximum adsorption level. As the solution pH is raised to range pH 4.0–6.0, the influence of H^+ is minimized and maximal Cu(II) uptake occurs.[35] However as the uptake of the Cu(II) increases significantly, an accumulation of positive charge on the adsorbent occurs producing repulsion among adjacent adsorption sites, thereby preventing other sites from actively binding with the metal also. The enhancement of metal adsorption at high anion concentrations may be brought about by cancellation of such repulsive charges by the presence of coadsorbing anions.

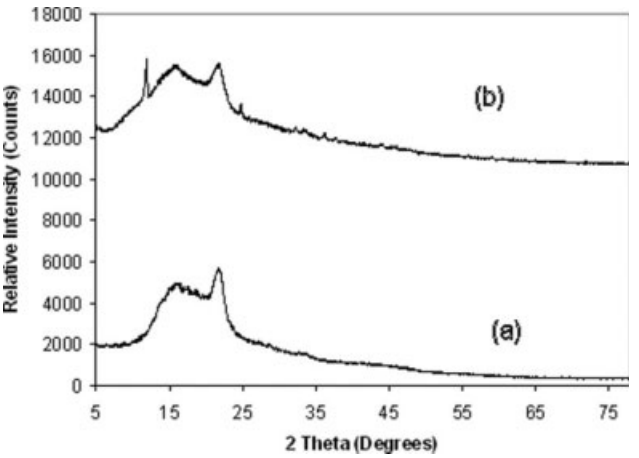

Figure 11 XRD spectra of (a) cellulose-*g*-GMA-imidazole and (b) Cu(II) loaded cellulose-*g*-GMA-imidazole.

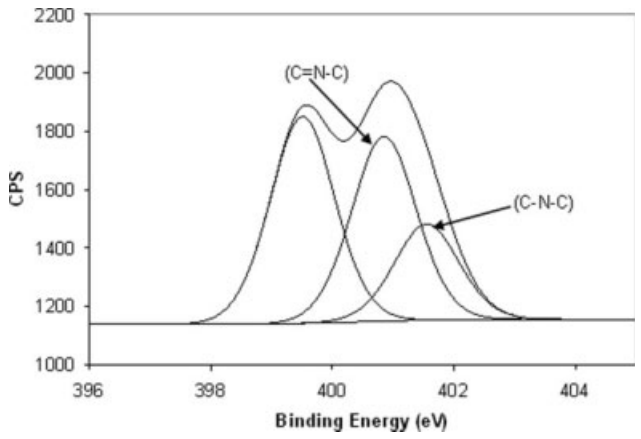

Figure 10 The N1s spectrum for Cu(II) loaded cellulose-*g*-GMA-imidazole.

CONCLUSIONS

An investigation into the sorbed state of Cu(II) on cellulose-*g*-GMA-imidazole was carried out. A number of analytical techniques were used to elucidate the nature of the binding between each metal and the cellulose-*g*-GMA-imidazole material. These techniques included SEM, EDX, FTIR, Raman spectroscopy and XRD.

SEM analysis revealed no significant differences between the morphological state of the parent cellulose-*g*-GMA-imidazole material and its metal bound form. However the use of the EDX technique provided clear evidence of the physical presence of copper on the cellulose-*g*-GMA-imidazole material. EDX analysis provided further evidence for the presence

of the sulphate anionic species on the cellulose-*g*-GMA-imidazole material post adsorption.

FTIR and Raman spectroscopy provided an insight into the extent to which perturbation of the imidazole ring occurred following adsorption of the metal on the cellulose-*g*-GMA-imidazole material. Subtle shifts in specific IR peaks at wavenumbers around 3112, 1232, 1512, and 1573 cm^{-1} were evident indicating the chelating effect of the imidazole in binding the copper metal.

XPS spectra clearly indicated the presence of the copper in the bound state. Further spectra clearly suggested the binding of Cu(II) ions to nitrogen atoms by the appearance of additional binding energy peaks for nitrogen on the cellulose-*g*-GMA-imidazole sample post adsorption. The highest binding energy occurred in the case of Cu(II).

While the FTIR and Raman spectroscopic work provided information on changes in the vibration of the imidazole ring following adsorption, XRD analysis of the cellulose-*g*-GMA-imidazole and the Cu(II) loaded cellulose-*g*-GMA-imidazole samples revealed a post adsorption change in crystallinity for the Cu(II) loaded cellulose-*g*-GMA-imdazole sample. This change in crystallinty may be attributable to adsorption of anions during the cation adsorption process. Specifically it appears that in the case of the Cu(II) adsorption the bound metal state contains some element of copper sulfate hydroxide ($Cu_3(OH)_4SO_4$ - antlerite). The XRD studies suggest that the overall adsorption process is a probably a combination of true chelation and surface precipitation of the polynuclear metal species.

The authors thank the help, support, and facilities of the Materials and Surface Science Institute at the University of Limerick.

References

1. Kamel, S.; Hassan, E. M.; El-Sakhawy, M. J Appl Polym Sci 2006, 100, 329.
2. O'Connell, D. W.; Birkinshaw, C.; O'Dwyer, T. F. Bioresource Technol 2008, 99, 6709.
3. Low, K. S.; Lee, C. K.; Mak, S. M. Wood Sci Technol 2004, 38, 629.
4. Marchetti, M.; Clement, A.; Loubinoux, B.; Gerardin, P. J Wood Sci 2000, 46, 331.
5. Aoki, N.; Fukushima, K.; Kurakata, H.; Sakamoto, M.; Furuhata, K. React Funct Polym 1999, 42, 223.
6. Saliba, R.; Gauthier, H.; Gauthier, R. Adsorp Sci Technol 2005, 23, 313.
7. Kubota, H.; Suzuki, S. Eur Polym Mater 1995, 31, 701.
8. Orlando, U. S.; Baes, A.; Nishijima, W.; Okada, M. Green Chem 2002, 4, 555.
9. Gupta, K. C.; Khandehar, K. J Appl Polym Sci 2002, 86, 2631.
10. Volesky, B.; Holan, Z. R. Biotechnol Prog 1995, 11, 235.
11. Ashkenazy, R.; Gottlieb, L.; Yannai, S. Biotechnol Bioeng 1997, 55, 1.
12. Benguella, B.; Benaissi, H.; Water Res 2002, 36, 2463.
13. Gyliene, O.; Rekertas, R.; Salkauskas, M. Water Res 2002, 36, 4128.
14. Li, N.; Bai, R. Sep Purif Technol 2005, 42, 237.
15. Liu, C.; Bai, R. J Membr Sci 2006, 284, 313.
16. Zhou, D.; Zhang, L.; Guo, S. Water Res 2005, 39, 3755.
17. Martinez, M.; Miralles, N.; Hidalgo, S.; Fiol, N.; Villaescusa, I.; Poch, J. J Haz Mater 2006, 133, 203.
18. Krishnani, K. K.; Xiaoguang Meng, C.; Christodoulatos, V.; Boddu, M. J Haz Mater 2008, 153, 1222.
19. Sun, B.; Mi, Z.; An, G.; Liu, G.; J Appl Polym Sci 2007, 106, 2736.
20. O'Connell, D.W.; Birkinshaw, C.; O'Dwyer, T. F. J Appl Polym Sci 2006, 99, 2888.
21. Langmuir, I. J Am Chem Soc 1918, 40, 1361.
22. Martell, A. E. Coordination Chemistry; Litton Educational Publishing Inc: New York, 1971; Vol. 1.
23. Verweij, P. D.; Sital, S.; Haanepen, M. J.; Driessen, W. L.; Reedijk, J. Eur Polym J, 1993, 29, 1603.
24. Kara, A.; Uzun, L.; Berirli, N.; Denizli, A. J Haz Mater, 2004, 106B, 93.
25. Wu, K. H.; Chang, T. C.; Wang, Y. T.; Hong, Y. S.; Wu, T. S. Eur Polym J 2003, 39, 239.
26. Sun, S.; Wang, L.; Wang, A. J Haz Mater 2006, 136, 930.
27. Sun, S.; Wang, A. React Funct Polym 2006, 66, 819.
28. Lippert, J. L.; Robertson, J. A.; Havens, J. R.; Tan, J. S. Macromolecules 1985, 18, 63.
29. Dambies, L.; Guimon, C.; Yiacoumi, S.; Guibal, E. Colloid Surf A 2001, 117, 203.
30. Xue, G.; Dai, Q.; Jiang, S. J Am Chem Soc 1988, 110, 2393.
31. Stumm, W.; Morgan, J. J. Aquatic Chemistry: Chemical Equilibria and Rates in Natural Waters, 3rd ed.; Wiley: New York, 1996.
32. Sengupta, A. K.; Zhu, Y.; Hauze, D. Environ Sci Technol 1991, 25, 481.
33. Muzarelli, A. A.; Rochetti, R. Talanta 1974, 21, 1137.
34. Navarro, R. R.; Sumi, K.; Matsumura, M. Water Sci Technol 1998, 38, 195.
35. O'Connell, D. W.Ph.D. Thesis, University of Limerick, 2007.